All-optical flip-flop in wideband PhC-based filter with Kerr saturable nonlinearity

**I.V. Guryev · I.A. Sukhoivanov · J.A. Andrade Lucio ·
E. Vargaz Rodriguez**

Abstract In the paper, we investigate dynamic properties of the wideband optical filter on the basis of nonlinear photonic crystal. An all-optical flip-flop using ultra-short pulses with duration lower than 200 fs is found in such filters and has been investigated. Switching on and switching off dynamics is considered in detail. There have been carried out studies of the stability of the PhC nonlinear filter with respect to variation of the operating wavelength and radiation intensity.

1 Introduction

Periodic structures recently known as photonic crystals (PhC) have been investigated and used for a long time as optical media providing control over the electromagnetic radiation. During the last two decades such periodic media of different kinds have been applied to optical data transmission (PhC optical fibers, fiber Bragg gratings, demultiplexers, dispersion compensators, etc.) and processing (integrated photonic chips, waveguides, laser micro-sources).

Photonic crystals containing optically nonlinear materials (i.e. nonlinear PhCs) have been known and widely investigated since 1990 [1, 2]. Bistability and localized modes in photonic superlattices with embedded layers possessing non-resonant cubic or Kerr-type nonlinearities have also been discussed in the literature [3–6]. Cascaded nonlinearities [7] demonstrate an effective way to lower the switching power by employing parametric interaction and frequency conversion in noncentrosymmetric quadratic nonlinear optical materials. Parametric interactions also allow propagation of spatial quadratic solitons [8]. The quadratic nonlinear photonic crystals have been introduced by Berger [9] in a study of multiwavelength frequency conversion in a plane geometry.

Particularly, tunable PhCs containing nonlinear materials have been investigated for a long time as a basis for all-optical telecommunications and data processing systems [10]. The bistability effect is also widely known in periodic structures, particularly due to the Fano resonance [11, 12] and in slow-light waveguides [13], due to defect-induced nonlinear transmission [14] and in coupled cavity waveguides [15]. However, most of the bistable structures investigated until now strongly depend on resonant properties of the optical structure and, therefore, are sensitive to structural defects. Moreover, high resonance quality of such structures does not allow them to process ultra-short optical pulses which hardly makes them applicable to high-speed data processing.

On the other hand, wideband PhC filters possess low resonance quality which provides the possibility to use them with ultra-short pulses [16] and, consequently, to design all-optical data processing devices on their basis.

Therefore, in this work we have investigated temporal response of the wideband PhC-based filter made of Kerr nonlinear materials. We have also demonstrated all-optical flip-flop in such filters achieved within a wide range of the radiation parameters and investigated their switch-on and switch-off dynamics.

The paper is organized as follows. In Sect. 2 we investigate temporal response of the nonlinear PhC to the continuous wave signal at different intensities and have made conclusion on the optimal intensity level for the specific filter. Section 3 is dedicated to investigation of the bistability

I.V. Guryev (✉) · I.A. Sukhoivanov · J.A. Andrade Lucio ·
E. Vargaz Rodriguez
Engineering Division, University of Guanajuato, Guanajuato,
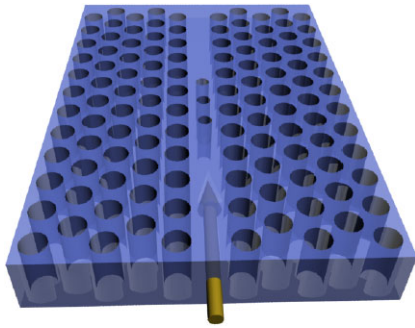Mexico
e-mail: guryev@ieee.org

Fig. 1 The structure of the investigated nonlinear PhC confined by the PhC waveguide

Fig. 2 Transmission of the filter as a function of the input intensity

effect of the structure excited by ultra-short pulses of different durations. In Sect. 4 we are demonstrating all-optical flip-flop in the filters with parameters previously determined in this work and analyze the conditions for the most effective switching-on and switching-off of the filter. Finally, in the last section we present the results of the investigation of the filters stability with respect to variation of the operating wavelength and the input radiation intensity.

2 Numerical analysis of nonlinear 2D photonic crystal

The schematic of investigated nonlinear PhC filter confined by the PhC waveguide is shown in Fig. 1. The period of the PhC with hexagonal lattice is $a = 0.37$ μm, the value of normalized radius is $r/a = 0.42$.

The PhC is made of chalcogenide glass of $Ag_{20}As_{32}Se_{48}$ possessing the refractive index of $n = 3.1$ and high optical nonlinear properties $n_2 = 9 \times 10^{-17}$ m^2/W [17].

The PhC filter is presented by three holes produced in the same PhC with $r/a = 0.35$, which makes its photonic bandgap (PBG) shifted with respect to the background PhC. The bandwidth of the filter refers to the spectral range corresponding either to transmission band or rejecting band. In case of the PhC filter presented in the paper, the rejecting bandwidth corresponding to the PBG is about 500 nm while the transmission bandwidth close to the PBG is about 100 nm with transmission $T \geq 0.5$. Taking into account spectral width of femtosecond pulses ($\delta\lambda \leq 50$ nm) the filter can be classified as wideband and it may provide low distortion of the ultra-short pulses passing through it [16].

Initially, the operating wavelength $\lambda = 1.05$ μm is selected to fall at the PBG of both background PhC and filter. However, due to optical nonlinearity the spectral characteristic of the filter appears to be shifted when increasing the radiation intensity.

The characteristics of the nonlinear PhC filter in this work are investigated by means of a numerical solution (namely, by the FDTD method) of Maxwell's equations [18].
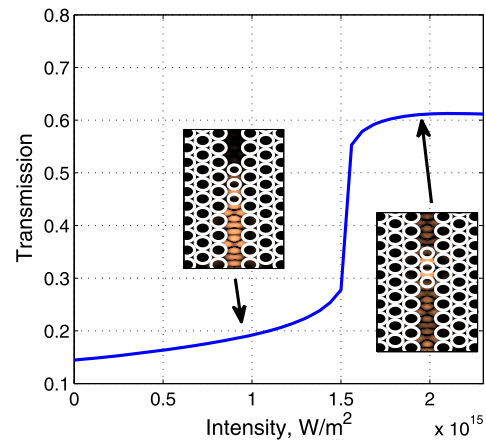
The reaction of the structure to increasing radiation intensity is presented in Fig. 2. The figure represents filter transmission as a function of the intensity of the CW monochromatic radiation. The insertions demonstrate the field behavior inside the waveguide with nonlinear PhC filter in case of low and high radiation intensity.

The results in Fig. 2 allow us to conclude that starting at a certain value of the intensity, the radiation wavelength appears outside the PBG which increases transmission of such a filter dramatically. The further growth of the nonlinearity no longer increases the transmission as is seen from Fig. 2 starting from $I = 1.7 \times 10^{15}$ W/m^2. Therefore, in our investigation we selected operating intensity below this value, namely, $I = 1.5 \times 10^{15}$ W/m^2.

3 Temporal response and bistability

Since the PhCs and, particularly, PhC-based filters possess resonant radiation transmission (the radiation is propagating from one element to another), the nonlinear spectrum shift requires a certain time which does not rely on response time of the nonlinear material. In order to investigate such a phenomenon, we carried out the study of temporal response of such a filter to Gaussian pulses of different durations. Each of the pulses in series possesses the same magnitude but different duration. The photorefractive properties of the materials remain the same for all pulses. This allows investigating only the contribution of the resonant processes inside the PhC into the bistability.

After the temporal response is obtained, it is represented in the form of the dependence of output intensity on the input one as presented in Fig. 3. The situation with the intensity growth corresponds to the lowest branch of the hysteresis loop, and lowering of the intensity stands for highest branch. In Fig. 3, the intensity variation direction is shown by arrows.

Fig. 3 Hysteresis loops at different durations of the Gaussian pulse: (**a**) $\tau = 50$ fs, (**b**) $\tau = 200$ fs, (**c**) $\tau = 400$ fs, (**d**) $\tau = 800$ fs
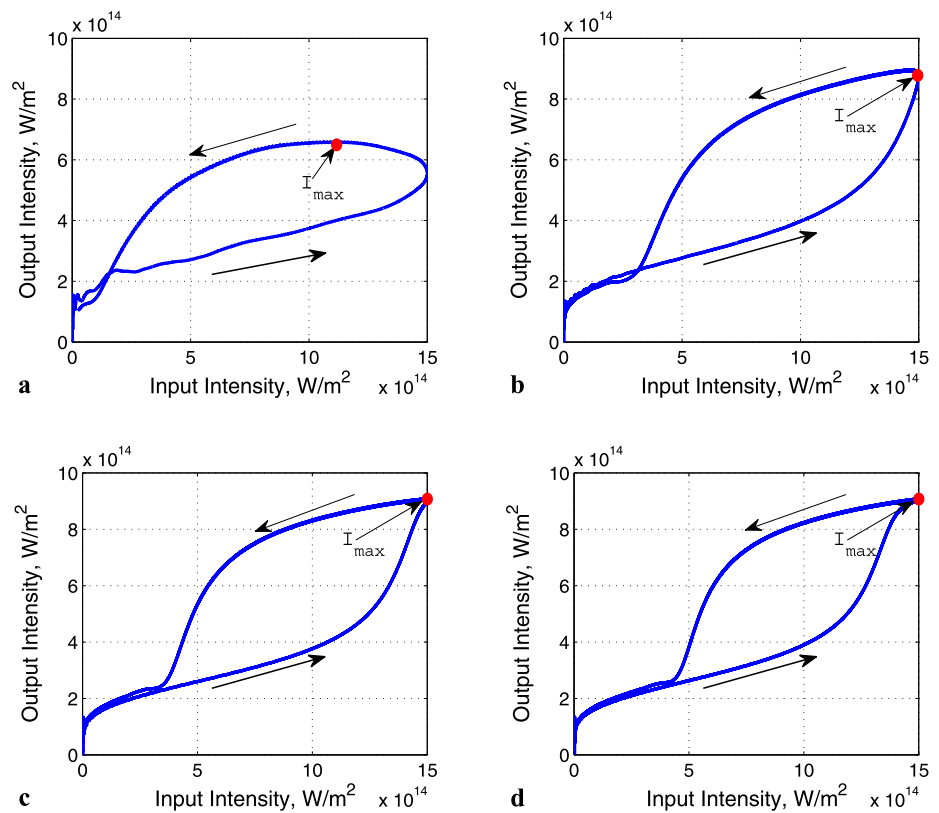
In case of linear optical materials, the branches coincide since no processes affect the properties of the PhC. However, in case of nonlinear materials the light trapped inside the filter due to resonances holds the refractive index of the nonlinear material and, consequently, the transmission of the filter, high, thus providing the difference in propagation of the leading and trailing edges of the pulse.

Due to finite saturation time of the resonances in the PhC, the minimum allowed pulse duration exists for a specific PhC filter. Normally, during the front edge of Gaussian pulse, the intensity inside the filter grows, which causes refractive index changes and, therefore, changes in the filter characteristic. However, if the pulse duration is lower than the time required to excite the eigen-state in the filter, significant nonlinear effects such as transmission growth appear after the input pulse maximum (see Fig. 3(a)). On the other hand, when the pulse duration is large, it is enough to excite the filter and, therefore, the maximum intensity of the input and output pulses coincide.

The problem may appear when the pulses with short duration are used in the system with strict synchronization. Due to specific behavior, it is quite difficult to synchronize such a pulse with other control pulses in the system and, therefore, the limits of the pulse duration should be considered. Moreover, the bistability contrast (i.e. difference between highest and lowest branches) for such a low duration pulses is lower than for ones with high duration.
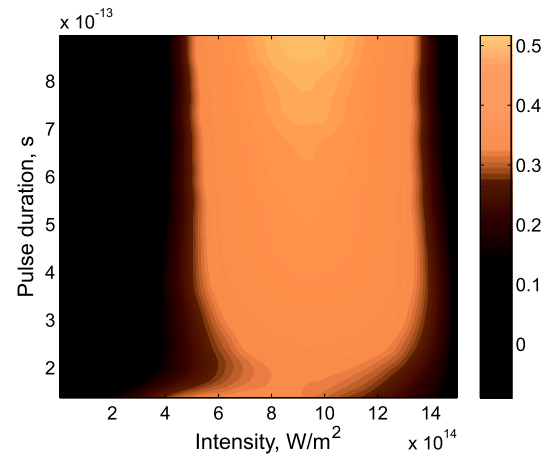

Fig. 4 Magnitude of the bistability as a function of the instant intensity and pulse duration

In order to find the time required for filter saturation, we have built the general characteristic of the magnitude of the bistability as a dependence on the pulse duration presented in Fig. 4. In the figure, the vertical axis corresponds to the pulse duration, while the horizontal one stands for the instant radiation intensity. Lights and shades in the figure indicate specific values of the difference between highest and

lowest branch of the hysteresis loop and is found from the following expression:

$$I' = \frac{(I_{\text{high}} - I_{\text{low}})}{I_{\text{max}}} \qquad (1)$$

The highest magnitude corresponds to the bright regions of the diagram while dark ones correspond to collapse of the loop.

Using this diagram it is possible to determine the saturation time of the wideband filter. Namely, the saturation time corresponds to the pulse duration at which the position of the maximum of the bistability contrast becomes constant i.e. when the maximum point of the highest branch of the characteristic presented in Fig. 3 coincides with maximum of the input intensity (see Fig. 3(b)). In case of our filter this minimum duration is $\tau = 180$ fs.

The characteristic indicates also the duration ranges where the bistability has maximum contrast ($\Delta t > 300$ fs), where the pulse duration is too low, the maximum of the characteristic is shifted into low-power region and the filter cannot be used as a bistable device ($\Delta t < 180$ fs) and the range where the bistability exists but its contrast is low ($180 < \Delta t < 300$ fs). Another important conclusion can be made from the diagram. The further growth of the pulse duration does not increase essentially the bistability contrast and, therefore, the wideband filter can be effectively used with ultra-short pulses as well as with CW signals.

Therefore, the study of the temporal responses carried out in the work demonstrates the possibility of all-optical switching of the filter by the pulses which increase the reduction of the intensity temporarily and, consequently, change the filter state.

4 Nonlinear switching by Gaussian pulses

After determining the possibility of control of the filter states by the ultra-short pulses, we have studied its nonlinear switching dynamics. For this reason the continuous wave pump signal is launched into the waveguide. Then, with certain delays, Gaussian control signals are launched which turn on and turn off the transmission of the filter. The power of the pump signal corresponds to the maximum magnitude of the hysteresis loop. Switching on occurs when the Gaussian signal is launched with the same phase as the pump one. If the signal possesses opposite phase, switching off occurs.

The temporal response of the investigated filter is demonstrated in Fig. 5. The upper figure shows the intensity of the pump signal. Figures 5(b) and 5(c) demonstrate turn on and turn off pulse sequences. In the lower figure, the resulting output signal is shown.

The pump signal intensity is slightly below the nonlinearity threshold. Therefore, switching on requires low intensity Gaussian pulse. On the other hand, when switching off, the
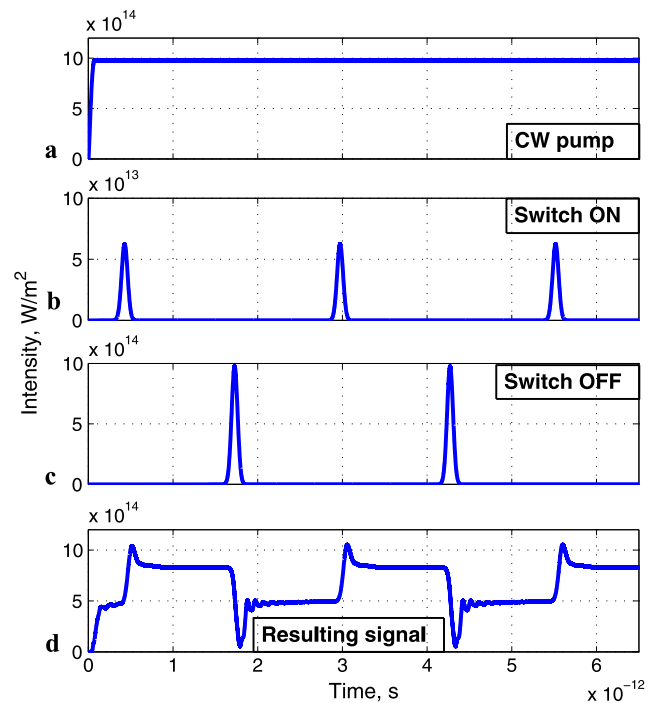

Fig. 5 The CW pump (**a**), on (**b**), off (**c**) and resulting signal (**d**)

signal intensity should be reduced down to 2×10^{14} W/m^2 as follows from Fig. 3(d). Therefore, the switching off signal maximum intensity is taken the same as that of the pump signal.

4.1 Switching ON dynamics

In Fig. 5(d) "zero" level of the temporal response corresponds to the intensity of 5×10^{14} W/m^2, while a level of "one" corresponds to 8×10^{14} W/m^2. Because of hysteresis behavior of the bistability, when switching on the pump and switching pulses should possess a total intensity high enough to initiate high transmission (particularly, in the current research, the maximum magnitude of the pump and switching on signal achieves 10^{15} W/m^2). Due to this, a little intensity splash takes place. As is shown in previous section, variation of the nonlinear PhC characteristic is not instant but requires a specific amount of time. In the case shown in Fig. 5(d) the leading edge of the switching on amounts to ≈ 100 fs. After the splash, a relaxation period is observed (≈ 300 fs). However, the comparison level is usually set below the steady level and, therefore, switching on may be considered as complete after the leading edge of the pulse.

The phase difference between the pump and control pulses are of crucial importance. In the left part of Fig. 6, the temporal response (horizontal axis) of the filter to the switch on signal is shown as a dependence of the phase mismatch. The mismatch is counted from the in-phase pump-switch pulse propagation. Bright regions of the figure correspond to high level of the intensity and the dark ones are for
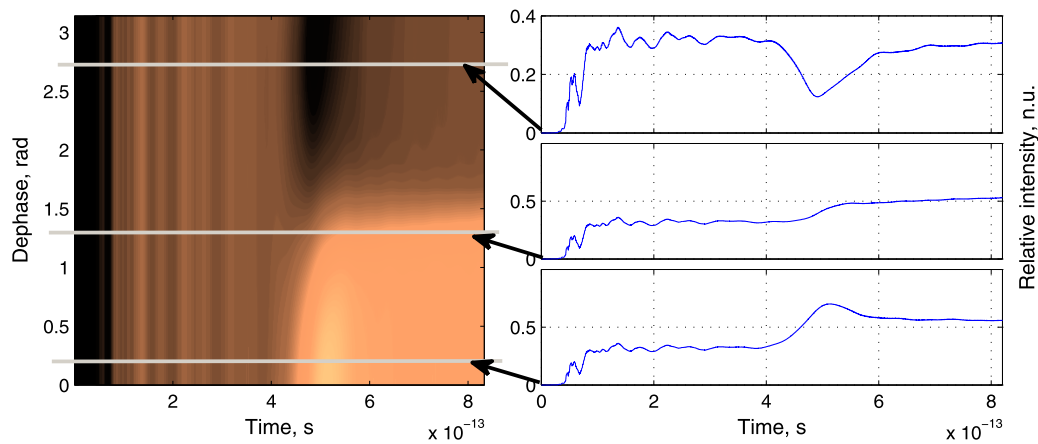
Fig. 6 Switching on dynamics in case of low and high phase mismatch of the signal
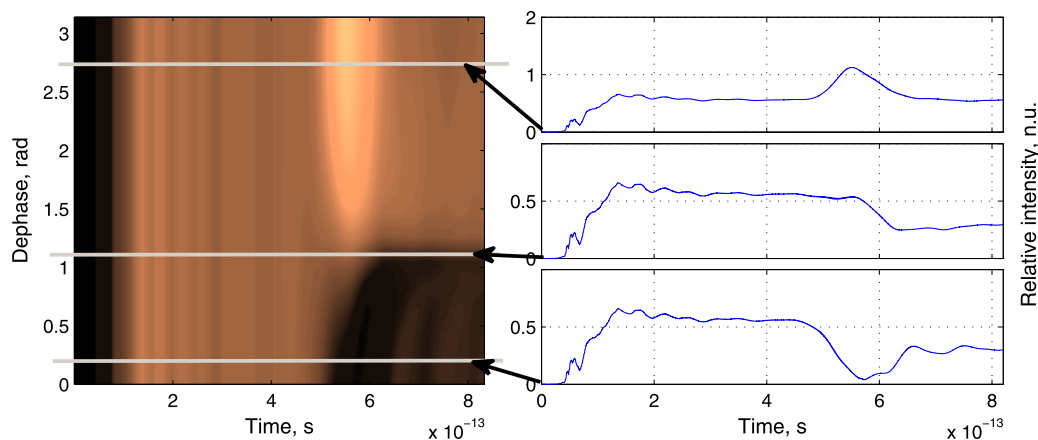

Fig. 7 Switching off dynamics in case of low and high phase mismatch of the signal

the low level. The slices of the characteristic are shown in the same figure to the right. As is seen from the figure, the phase matching conditions (when the control signal causes switching on) cover almost $\pi/2$ of the whole phase, which is almost 50% of the period. Such a big range of the phase matching provides a low error probability when switching on.

4.2 Switching off dynamics

Similar to switching on, the switching off requires phase of the control pulse to have strict correspondence to the pump one. To investigate this side of the problem the characteristics similar to the one presented in Fig. 6 have been computed for the case of switching the filter off (see Fig. 7). However, in this case zero phase mismatch corresponds to the control pulse phase which is opposite to the pump one.

In case of switching off, the range of allowed phase mismatch is lower than in case of switching on. It covers $\pi/3$ radians, which is less than 40% of the period and, consequently, the off pulse should be launched more accurately.

Moreover, the switching off time is sensitive to the phase mismatch. When the phases are strictly opposite (phase shift between the pump and the control is $\pi + 2\pi n$, where n is integer), the switching off time is about 500 fs due to relaxation oscillations (see the right bottom part of Fig. 7). In case of low phase mismatch, the transient period is lower and, correspondingly, the switching off time is reduced to 100 fs as is seen in the right middle part of Fig. 7.

Switching off is absent only when the phase mismatch becomes large (see the top right part of Fig. 7). Moreover, if the filter is initially in lower state, it may become switched on.

5 Stability of the wideband filter

As it have been mentioned previously in this paper, we use wideband optical filter as a bistable element. Due to the fact that such filters characteristics do not depend strictly on the resonant properties (in contrast to high-Q filters), such filter should possess high stability with respect to wavelength
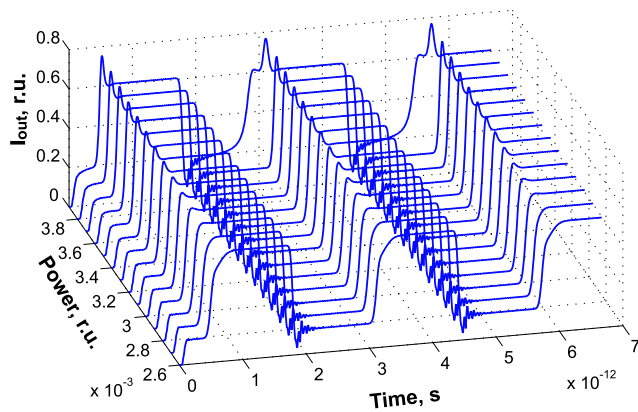
Fig. 8 The flip-flop characteristics computed at different power levels
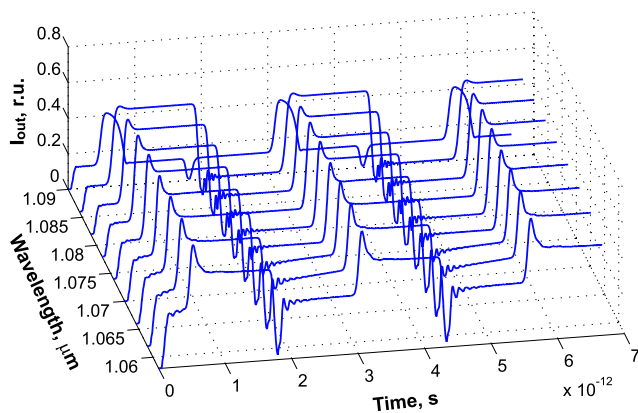

Fig. 9 The flip-flop characteristics computed within the range of wavelength

variation as well as to the power variation. Here we investigating this property of the filter.

First, we have computed the flip-flop characteristics similar to the ones presented in Fig. 5 but taken at different pump wave intensity (see the series of the characteristics in Fig. 8). The lowest power corresponds to the one which still provides switching on and allows the higher level to exist long enough. Then we raise the power until the low level stability appears broken.

We have found that the filter is functional within 30% of power variation.

On the other hand, we have investigated the stability of the filter with respect to the wavelength variation. We have computed the flip-flop characteristic at different radiation wavelength (see Fig. 9). Increasing the wavelength we are moving away from the PBG edge, and, therefore, more power is required to shift the spectrum enough to provide the bistability effect.

In contrast to previous case, at high wavelength shift the highest level becomes unstable and the structure is unable to switch on. Nevertheless, due to wide bandwidth of the

filter, the deviation of 30 nm do not affect essentially the characteristic.

The deviation of the power and the wavelength causes slight variation of the switching on and switching off time. The largest switching on time is observed at low power when the intensity of the pulse is not enough to switch the structure on, however, its enough to perturb the structure and break the equilibrium of the bottom state. After this, the transmission of the filter will grow slowly until it achieves maximum transmission according to hysteresis loop (see Fig. 3(d)).

On the other hand, the lowest switching on time corresponds to the largest deviation of the wavelength, i.e. when the operating wavelength is far enough from the edge of the PBG, and switching requires exactly the amount of energy provided by the switching pulse.

As for switching off time, since the intensity is always reduced almost to zero by the anti-phase pulse, the amount of time required for this operation remains unchanged or varies insignificantly as compared with switching on time, independently on power or wavelength deviation.

Therefore, the stability of the filters demonstrated during this study, cannot possibly be achieved using high-Q resonant filters.

6 Conclusion

The bistability effect has been theoretically predicted in the microstructures represented by the wideband optical PhC-based filters with third-order Kerr nonlinearities for the CW radiation or the ultra-short pulses down to 180 fs of duration. Numerical experiments have shown the possibility of an all-optical flip-flop with pulses of 200 fs of duration which makes such a filters suitable for a high-speed all-optical data processing unit. Particularly, we considered in detail the switching on and switching off dynamics of the investigated filters and found a possible dephase at which the switching is still possible.

Main drawback of the proposed filters is the phase matching requirements between the pump and the switching signals, which is quite difficult to implement in micro-devices. However, the problem may be solved by creating specially optimized auxiliary waveguides which is outside of current paper consideration.

Another problem which may arise when implementing the wideband nonlinear filter presented in the work is the power required to induce a high refractive index change and, consequently, to shift the PBG edge. The problem will be solved with the optimization of the filter design as well as the one of the waveguide. The optimization aim is to develop the filter with a sharp PBG edge which will provide high transmission changes with low intensity variation.

References

1. S. Larochelle, Y. Hibino, V. Mizrahi, G.I. Stegeman, Electron. Lett. **26**, 1459 (1990)
2. M. Scalora, J.P. Dowling, C.M. Bowden, M.J. Bloemer, Phys. Rev. Lett. **73**, 1368 (1994)
3. C.T.Q. Li, K.M.H. Chan, C.M. Soukoulis, Phys. Rev. B **53**, 577 (1996)
4. E. Lidorikis, Q. Li, C.M. Soukoulis, Phys. Rev. B **54**, 10249 (1996)
5. E. Lidorikis, K. Busch, Q. Li, C. Chan, C.M. Soukoulis, Phys. Rev. B **56**, 15090 (1997)
6. D. Hennig, G.P. Tsironis, Phys. Rep. **307**, 333 (1999)
7. G.I. Stegeman, D.J. Hagan, L. Torner, Opt. Quantum Electron. **28**, 1691 (1996)
8. Y.S. Kivshar, *Advanced Photonics with Second-Order Optically Nonlinear Processes* (Kluwer, Dordrecht, 1999)
9. V. Berger, Phys. Rev. Lett. **81**, 4136 (1998)
10. S.F. Mingaleev, Y.S. Kivshar, Opt. Photonics News **49** (2002)
11. S.F. Mingaleev, A.E. Miroshnichenko, Y.S. Kivshar et al., Phys. Rev. E **74**, 046603 (2006)
12. S.F. Mingaleev, A.E. Miroshnichenko, Y.S. Kivshar, Opt. Express **15**, 12380 (2007)
13. L. Dai, C. Jiang, J. Lightwave Technol. **28**, 905 (2010)
14. M.W. Feise, I.V. Shadrivov, Y.S. Kivshar, Appl. Phys. Lett. **85**, 1451 (2004)
15. W. Ding, L. Chen, S. Liu, Opt. Commun. **265**, 500 (2006)
16. I. Sukhoivanov, I. Guryev, O. Shulika et al., J. Optoelectron. Adv. Mater. **8**, 1626 (2006)
17. K. Ogusu, J. Yamasaki, S. Maeda, M. Kitao, M. Minakata, Opt. Lett. **29**, 265 (2004)
18. A. Taflove, S. Hagness, *Computational Electrodynamics: The Finite-Difference Time-Domain Method*, 3 edn. (Artech House, Norwood, 2005)